Equilibrium and Kinetic Folding of Hen Egg-White Lysozyme Under Acidic Conditions

Kenji Sasahara,* Makoto Demura, and Katsutoshi Nitta
Division of Biological Sciences, Graduate School of Science, Hokkaido University, Sapporo, Hokkaido, Japan

ABSTRACT **The equilibrium and kinetic folding of hen egg-white lysozyme was studied by means of circular dichroism spectra in the far- and near-ultraviolet (UV) regions at 25°C under the acidic pH conditions. In equilibrium condition at pH 2.2, hen lysozyme shows a single cooperative transition in the GdnCl-induced unfolding experiment. However, in the GdnCl-induced unfolding process at lower pH 0.9, a distinct intermediate state with molten globule characteristics was observed. The time-dependent unfolding and refolding of the protein were induced by concentration jumps of the denaturant and measured by using stopped-flow circular dichroism at pH 2.2. Immediately after the dilution of denaturant, the kinetics of refolding shows evidence of a major unresolved far-UV CD change during the dead time (<10 ms) of the stopped-flow experiment (burst phase). The observed refolding and unfolding curves were both fitted well to a single-exponential function, and the rate constants obtained in the far- and near-UV regions coincided with each other. The dependence on denaturant concentration of amplitudes of burst phase and both rate constants was modeled quantitatively by a sequential three-state mechanism, U↔I↔N, in which the burst-phase intermediate (I) in rapid equilibrium with the unfolded state (U) precedes the rate-determining formation of the native state (N). The role of folding intermediate state of hen lysozyme was discussed. Proteins 2002;49:472–482.**

Key words: hen egg-white lysozyme; protein folding; stopped flow; folding intermediate

INTRODUCTION

To understand how unfolded protein can rapidly adopt a unique, densely packed, three-dimensional structure is one of the major goals in folding studies.[1] An important aspect of experimental studies of protein folding has been the detection and characterization of partially folded states, including intermediates that are stable at equilibrium and transient intermediates observed in kinetic experiments.[1–3] For several proteins, partially folded equilibrium intermediates are populated under mildly denaturing conditions and are characterized as molten globule states.[2–4] Experimental studies of these non-native states have shown that they have particularly intriguing conformational properties; most notably, they are compact with substantial secondary structure and an overall native-like fold.

Because some of the kinetic burst-phase intermediates, observed just after the dead time in protein-refolding experiments, have been shown to resemble equilibrium intermediates, a sequential model has been proposed, in which folding from the unfolded state (U) to the native state (N) proceeds along a sequential pathway, U→I→N, with at least one obligatory intermediate (I).[2–4] In this model, partially folded intermediates would play an essential role in the folding process by restricting the conformational space accessible to the polypeptide chain. In contrast to this picture, the folding of small proteins has been described to fold rapidly and efficiently without accumulation of detectable intermediates in an apparent two-state folding reaction.[5] In addition, it has been suggested that the intermediate state like molten globule is not obligatory in folding reaction but may be misfolded structure trapped in local energy minima.[6,7] As a consequence, the significance of intermediate states in protein folding is still the subject of debate.[8–10]

Hen egg-white lysozyme is a small globular protein of 129 residues and has four disulfide bonds, which are left intact in the present studies. Equilibrium and kinetic folding of this protein under the neutral pH conditions has been studied in great detail by a combination of different techniques.[11–31] Earlier kinetic studies on hen lysozyme, based on optical probes and hydrogen exchange-labeling method, revealed a complex folding mechanism with multiple pathways.[18] Kinetic CD measurements in the far-ultraviolet (UV) have been informative about the early steps in the folding of this protein.[15,18] The results have indicated that substantial secondary structure is formed within the stopped-flow dead time, and subsequent time course is complex and shows fast and slow phases. During the fast phase of refolding, there was a further decrease in the ellipticity, which is considerably more negative than the corresponding ellipticity of native lysozyme (overshoot). The native value was then regained in the slow phase.

Abbreviations: GdnCl, guanidinium chloride; CD, circular dichroism; N, native; I, intermediate; U, unfolded.

K. Sasahara's present address is Section of Physical Biochemistry, National Institute of Diabetes, Digestive, and Kidney Disease, National Institutes of Health, Bethesda, MD 20892.

*Correspondence to: Kenji Sasahara, Building 8, Room 220, National Institutes of Health, Bethesda, MD 20892. E-mail: Kenjisa@intra.niddk.nih.gov

Received 8 February 2002; Accepted 30 May 2002

Moreover, interrupted refolding experiments of this protein at neutral pH have clearly shown that the existence of parallel folding pathways, in which most molecules refold along a relative slow kinetic pathway through a well-populated transient intermediate, whereas about 15% of the molecules fold directly to the native state without populating the intermediate.[23,26] In the parallel folding model, whether the partially structured intermediate states facilitate folding or, conversely, slow the folding process by the kinetic traps and high-energy barriers remain unclear.[9] Thus, to elucidate the role of the kinetic intermediate and the origin of the slow pathway of hen lysozyme folding is an important step toward unraveling the mechanism of protein folding.

Hen lysozyme shows an equilibrium intermediate under strongly acidic conditions as well as a kinetic intermediate state.[13,29] In addition, the refolding curves under acidic conditions by the far-UV CD could be fitted to a single exponential process without the overshoot observed at neutral pH.[15] Moreover, reducing pH leads the much longer lifetime of the burst-phase species than that at well-studied higher pH values.[31] To clarify the role and significance of the partially folded intermediate that transiently accumulates during hen lysozyme folding and its possible relationship with the partially folded equilibrium intermediate, we have investigated the GdnCl-induced equilibrium and kinetic folding of hen egg-white lysozyme by means of CD spectroscopy at 25°C under the acidic pH condition.

MATERIALS AND METHODS

Materials

Hen egg-white lysozyme (crystallized six times) was purchased from Seikagaku Corporation, Ltd., Tokyo, Japan, and used without further purification. Biochemical grade GdnCl was purchased from Wako Pure Chemical Industries, Ltd., Japan. Potassium chloride and hydrochloric acid were analytical grade (Junsei Chemical Industries, Ltd., Japan), and distilled, deionized water was used for preparing solutions.

Equilibrium Experiments

The stock solutions of native protein in buffer and unfolded protein in about 6 M GdnCl were prepared, respectively. Both stock solutions, which contain 0.6 M KCl, were adjusted to pH 2.2 or pH 0.9 by adding HCl with HORIBA pH meter M-8s. The concentration of lysozyme in both stock solutions was about 0.4 mg/mL and determined by measuring the absorbance at 280 nm using an extinction coefficient of $E_{1\%} = 24.5$. The concentration of GdnCl was determined by the difference between the refractive index of GdnCl solution and GdnCl-free solution.[32] The two stock solutions were then mixed in the appropriate ratios to prepare 30 sample solutions at the desired concentrations of GdnCl. These sample solutions were incubated at room temperature for 15 h. Equilibrium experiments were conducted in a Jasco J-725 spectropolarimeter (Japan Spectroscopic Co., Ltd., Japan). In the GdnCl-induced equilibrium unfolding of lysozyme, ellipticities at 289 nm and 222 nm were measured in quartz cells with 10 mm and 1 mm path lengths, respectively. The temperature surrounding the cell was maintained at 25 ± 0.1°C by circulating an ethylene glycol + water mixture from a constant-temperature bath.

Kinetic Experiments

All measurements were made by using a stopped-flow apparatus (specially constructed by Unisoku, Inc., Osaka, Japan; volume ratio 1:10) attached to the spectropolarimeter (Jasco J-725). The path length of 4 mm with a dead time of <10 ms was used for far- and near-UV CD measurements. The temperature in the stopped-flow unit was maintained at 25 ± 0.1°C by circulating water. The time course of refolding and unfolding of hen lysozyme in various GdnCl concentrations was followed by monitoring changes of the near- and far-UV CD as a function of time. The final protein concentrations in the observation cell were about 0.1 and 1.0 mg/mL for far- and near-UV studies, respectively, and were checked by measuring the absorbance at 280 nm. The final GdnCl concentration was also checked by measuring the refractive index of the solutions collected in each experiment. All the solutions contained 0.6 M KCl/HCl at pH2.2. Each experiment was repeated 3–50 times, and the accumulated kinetic data were averaged. The kinetic data were fitted by the nonlinear least-squares method to the Eq. 1:

$$A(t) = A(\infty) + \Delta A \exp(-k_{app}t) \quad (1)$$

where $A(t)$ and $A(\infty)$ are the observed values of the CD ellipticity values at time t and the infinite time, respectively, and ΔA and k_{obs} are the amplitude and the apparent rate constant of the observed phase, respectively.

RESULTS

Equilibrium Unfolding

Figure 1 shows the GdnCl-induced equilibrium unfolding transition curves of hen lysozyme at pH 2.2 (A) and pH 0.9 (B), monitored by CD ellipticity at 222 nm in the far-UV region and at 289 nm in the near-UV region. The former provides information on the organization of secondary structure, and the latter is associated principally with the six tryptophan residues, reflecting the tertiary structure. The equilibrium data were preliminarily fitted by nonlinear least-squares analysis by using the two-state model, based on linear free energy relationship[33,34]:

$$\Delta G_{NU} = \Delta G^0_{NU} - m_{NU}c \quad (2)$$

where ΔG_{NU} is the free energy of unfolding, ΔG^0_{NU} is ΔG_{NU} at 0 M GdnCl, c is the denaturant concentration, and m_{NU} is the cooperative index of the transition, respectively. The observed ellipticity (A_{obs}) at any concentration of GdnCl is given by the following equation:

$$A_{obs}(c) = [A_N + A_U \exp\{-(\Delta G^0_{NU} - m_{NU}c)/RT\}]/ [1 + \exp\{-(\Delta G^0_{NU} - m_{NU}c)/RT\}] \quad (3)$$

where R and T are the gas constant and the absolute temperature, respectively. A_N and A_U are ellipticity values

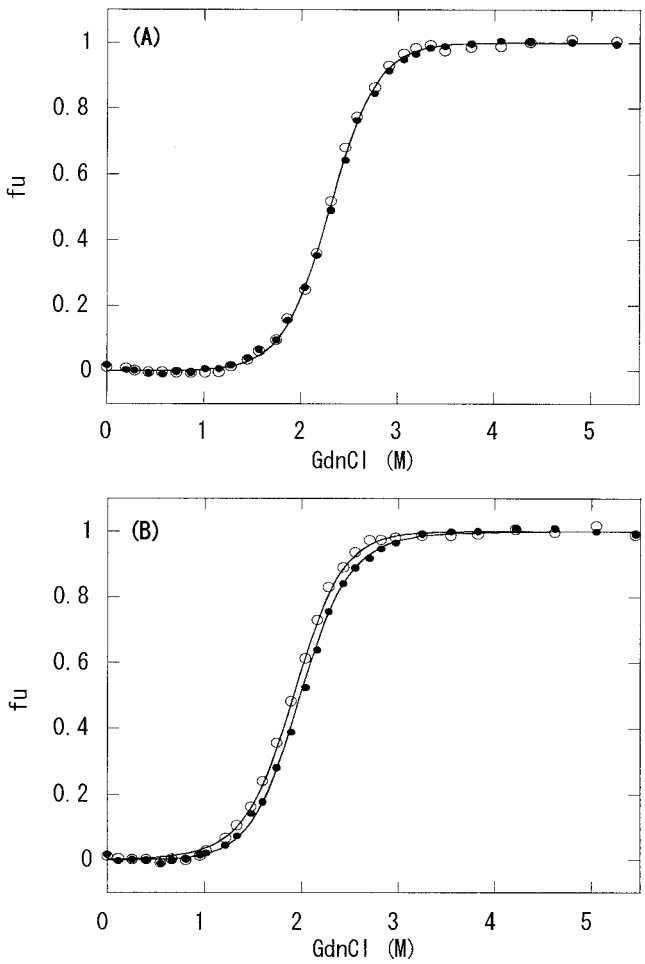

Fig. 1. GdnCl-induced equilibrium unfolding transition of hen lysozyme at (**A**) pH2.2 and (**B**) pH0.9, estimated from ellipticities at 289 nm (open circle) and at 222 nm (filled circle). The data are shown in terms of the fraction of unfolded protein at each GdnCl concentration according to Eq. 4. Continuous lines in (A) and (B) represent the best fit of each data set to a two-state model based on Eq. 3 and the three-state transition model based on Eq. 5, respectively. In the three-state analysis at pH 0.9, it was assumed that $f_N = 1-f_{app,289}$, $f_I = f_{app,289}-f_{app222}$, and $f_U = f_{app,222}$, where f_N, f_I, and f_U are the fractions of the three states ($f_N + f_I + f_U = 1$), and $f_{app,289}$ and $f_{app,222}$ are apparent fractions of unfolded protein monitored by near- and far-UV CD at 289 and 222 nm, respectively.

in the N and the U states, respectively, which are assumed to be linearly dependent on c ($A_N = a_1 + a_2c$ and $A_U = a_3 + a_4c$. In this analysis, six parameters are used to fit the data; ΔG^0_{NU}, m_{NU}, and $a_1 \sim a_4$. Data in Figures 1(A) and (B) are plotted as the fraction of unfolded protein, f_u, versus the concentration of GdnCl according to Eq. 4:

$$f_u = (A_N - A_{obs})/(A_N - A_U)$$
$$= (a_1 + a_2c - A_{obs}(c))/(a_1 + a_2c - a_3 - a_4c) \quad (4)$$

In equilibrium condition at pH 2.2, the transition curves obtained in both wavelength regions coincide, indicating that tertiary and secondary structures of the protein unfold simultaneously in a cooperative process. As a result, the GdnCl-induced unfolding of hen lysozyme at pH 2.2 was fitted to a two-state transition model. In more acidic condition (pH 0.9), however, the two transition curves no longer coincide [Fig. 1(B)], indicating the existence of at least one partially folded equilibrium state in the unfolding process. This result is in complete agreement with the previous GdnCl-induced unfolding experiment at pH 0.9.[29]

To analyze the GdnCl-induced transition curves at pH 0.9, we assumed a three-state transition model where three states (i.e., the native (N), the intermediate (I), and the unfolded (U) states) are required for interpreting the transition curves. On the basis of this assumption, the observed ellipticities of the protein [$A_{obs}(c)$] at any concentration of the denaturant are given by the following equation:

$$A_{obs}(c) = [A_N + A_I \exp\{-(\Delta G^0_{NI} - m_{NI}c)/RT\}$$
$$+ A_U \exp\{-(\Delta G^0_{NU} - m_{NU}c)/RT\}]/[1 + \exp\{-(\Delta G^0_{NI}$$
$$- m_{NI}c)/RT\} + \exp\{-(\Delta G^0_{NU} - m_{NU}c)/RT\}] \quad (5)$$

where A_N, A_I, and A_U are the ellipticity values of the N, I, and U states, m_{NI} and m_{NU} represent the cooperative indexes of the respective transitions, and ΔG^0_{NI} and ΔG^0_{NU} are ΔG_{NI} and ΔG_{NU} at 0 M GdnCl, respectively. The CD data of Figure 1(B) were analyzed on the basis of Eq. 5 by the nonlinear least-squares method. In the analysis, we performed the global fitting, in which the transition curves at different wavelengths (222 and 289 nm) were fitted simultaneously by using the A_N and A_U values obtained by Eq. 3, on the assumption that A_N equals A_I in the transition curve detected at 222 nm, and A_I equals A_U in that detected at 289 nm, respectively. This assumption seems to be reasonable according to the following facts: (i) the ellipticity at 222 nm gives native-like values in the molten globule state; (ii) the ellipticity at 289 nm monitors aromatic groups in specific orientations fixed through tertiary interactions so that spectra of unfolded and molten globule states are characterized by an almost complete absence of CD intensity at this wavelength.[13,29] These facts were also confirmed in the burst-phase intermediate populated rapidly during refolding of this protein as described below. The fitting variables in the least-squares analysis were thus two sets of ΔG^0_{NI}, ΔG^0_{NU}, m_{NI} and m_{NU} for the transition curve at the two different wavelengths (222 and 289 nm). The best-fit values of the equilibrium unfolding parameters at pH 2.2 and 0.9 are given in Table I. The continuous lines in Figures 1(A) and (B) represent the theoretical curves drawn with the parameter values in Table I.

In addition, we have compared the two-state and the three-state analyses for the transition curves obtained at pH 0.9 to see whether there is a significant deviation from the two-state behavior. Figure 2 provides the deviation from the two-state fit for the unfolding data at pH 0.9. A small but significant deviation is seen between the two transition curves monitored at 289 and 222 nm. The deviation from the two-state fit is well represented by the three-state fit in which only N, I, and U states are populated. As a result, the GdnCl-induced equilibrium transition curves of hen lysozyme at pH 2.2 and 0.9 are

TABLE I. Equilibrium Unfolding Parameters of Hen Egg-White Lysozyme at 25°C

pH	ΔG^0_{NU} (kJ/mol)	m_{NU} (kJ/mol/M)	ΔG^0_{NI} (kJ/mol)	m_{NI} (kJ/mol/M)	ΔG^0_{IU} (kJ/mol)	m_{IU} (kJ/mol/M)
2.2[a]	24.22 (0.6)	10.57 (0.25)				
0.9[b]	20.24 (1.05)	10.36 (0.64)	15.17 (2.71)	5.29 (1.96)	5.07 (1.27)	5.07 (1.88)

[a]The parameters were estimated on the basis of a two-state mechanism (Eq. 3).
[b]The parameters were estimated on the basis of a three-state mechanism (Eq. 5).

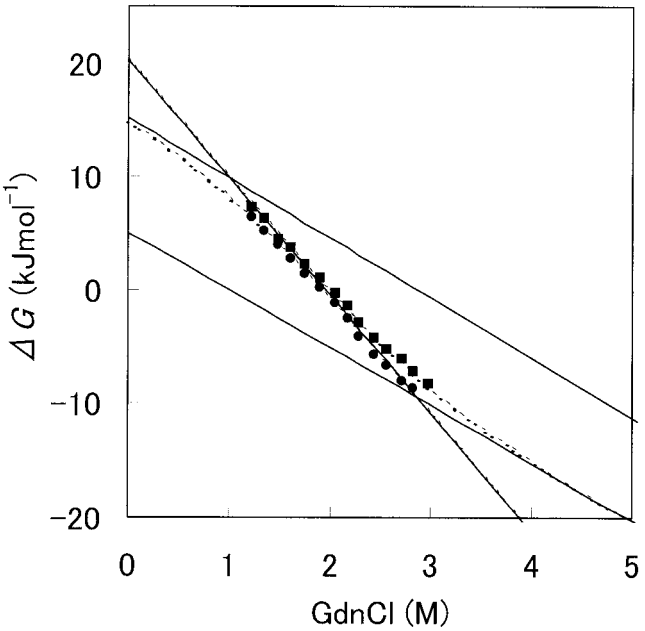

Fig. 2. Deviation from the two-state fit for the GdnCl-induced unfolding data at pH 0.9. Filled circles and filled squares represent ΔG_{NU} values of the two transition curves monitored by CD ellipticities at 289 and 222 nm, respectively, in which ΔG_{NU} values were calculated on the basis of the two-state transition model. The dotted lines through ΔG_{NU} values represent the nonlinear least-squares fit to the experimental data. The linear solid lines represent ΔG_{NU}, ΔG_{NI}, and ΔG_{IU} values drawn with the parameter values in Table I.

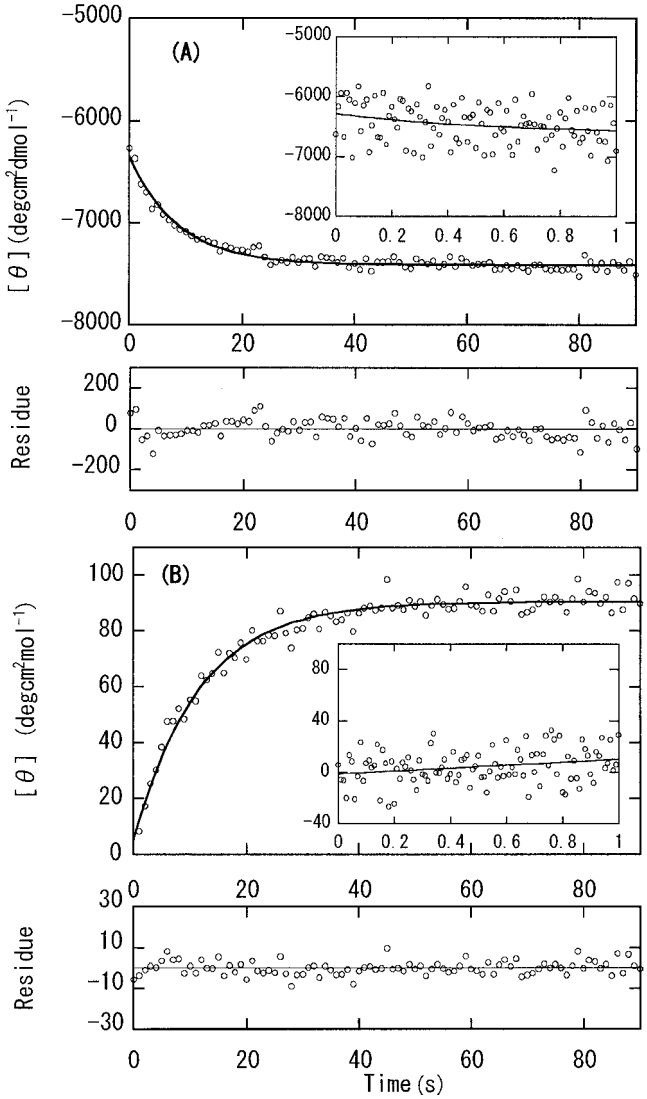

Fig. 3. Representative time courses of folding at pH 2.2 of the hen lysozyme monitored by CD at (**A**) 222 nm and (**B**) 289 nm. The reaction was initiated by a GdnCl concentration jump from 6.0 to 1.35 M. The insets show the refolding curves within 1 s. The continuous lines show the best fit of these data to single exponential functions. The lower panels show the difference between the observed values and fitted curves.

well represented by the two-state and three-state mechanisms, respectively.

Kinetics of Folding and Unfolding Reactions

Stopped-flow CD experiments were conducted to investigate the kinetics of folding and unfolding reactions of hen lysozyme at pH 2.2. The refolding reactions were induced by concentration jumps of GdnCl from 6.0 M to various concentrations by the stopped-flow mixing technique, and the resultant kinetics were observed by CD measurements at 222 and 289 nm. Figures 3(A) and (B) show representative refolding traces of hen lysozyme. After completion of the refolding, the ellipticities at 289 and 222 nm were consistent with those measured at equilibrium, showing that the unfolding/refolding transition of this protein is reversible. In the acidic pH condition, the overshoot in the far-UV CD observed at neutral pH was not observed, and the visible part of the kinetics (i.e., after the dead time) was much slower than that at neutral pH.[15] As can be seen in Figure 3, a significant fraction of the total far-UV CD change occurs during the dead time (<10 ms) of the stopped-flow apparatus (burst phase), indicating that extensive secondary structure is formed within the dead time of stopped-flow experiment. On the other hand, when monitored by the near-UV CD, the burst phase was not observed. Both the refolding curves could be fitted to a single exponential process, consistent with a single rate-limiting activation barrier.

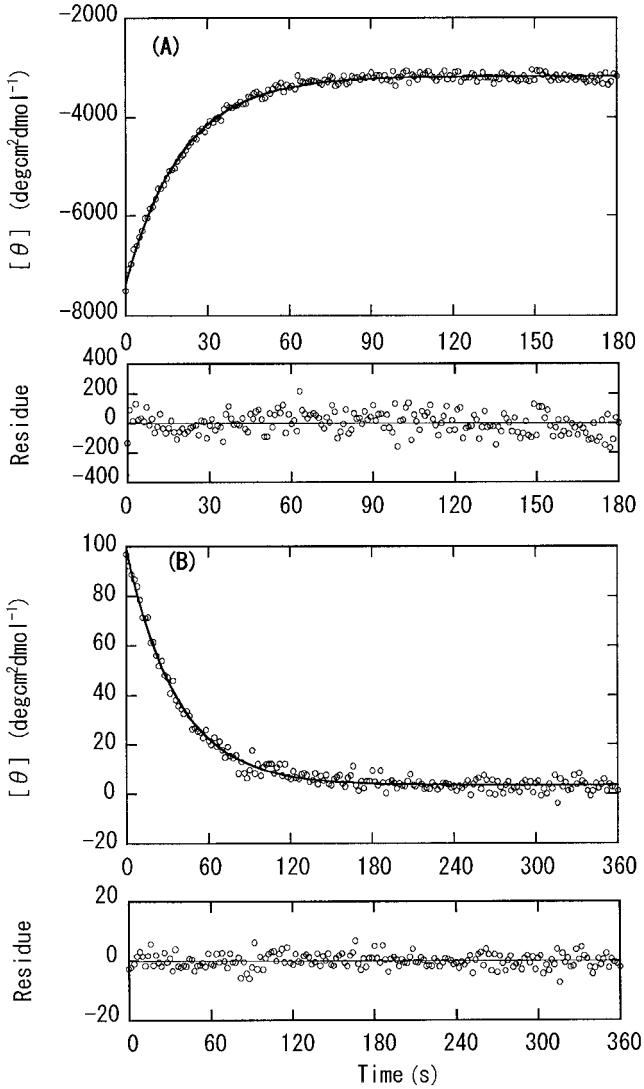

Fig. 4. Representative time courses of unfolding at pH 2.2 of hen lysozyme monitored by CD at (**A**) 222 nm and (**B**) 289 nm. The reaction was initiated by a concentration jump of GdnCl from 0 to 4.46 M (**A**) and from 0 to 4.13 M (**B**). The data shown together with the residuals represent the fit of the data to a single exponential process.

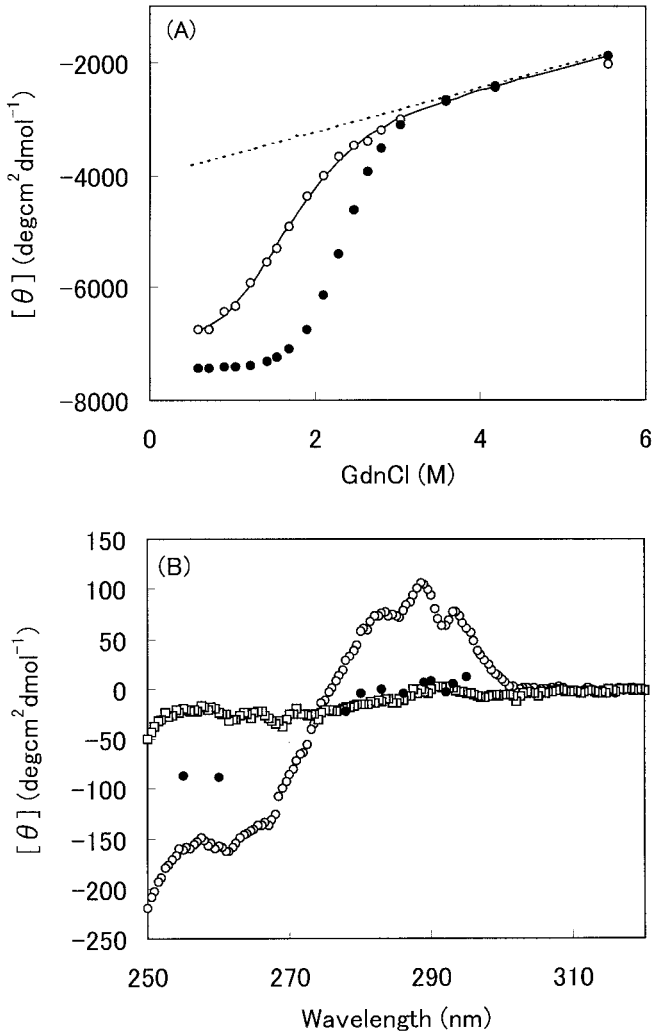

Fig. 5. **A:** The GdnCl-induced unfolding transition curve at pH 2.2 of the burst-phase intermediate measured by the CD ellipticity at 222 nm. Open circles represent the burst-phase amplitudes obtained by the extrapolation to zero time of the kinetic refolding curve measured under the corresponding GdnCl concentration. Filled circles represent final CD intensities observed during the refolding process. The dotted line shows the CD signal expected for the unfolded state assuming that it changes linearly with denaturant concentration. The solid line represents the best fit of the data to the on-pathway model (Eq. 12), which describes a two-state transition between the burst-phase intermediate and the unfolded state. **B:** CD spectra of hen lysozyme in the near-UV region at pH 2.2. The CD spectra of hen lysozyme in the native (0.55 M GdnCl; open circles) and the unfolded state (6.0 M GdnCl; squares) are shown. Filled circles show the ellipticity values obtained by extrapolating the observed kinetic traces to zero time, in which the reactions were induced by concentration jumps of GdnCl from 6.0 to 0.55 M.

The time-dependent unfolding reactions of the protein, induced by concentration jumps from 0 M to different final GdnCl concentrations ranging from 2.6 to 5.4 M, was monitored by stopped-flow CD at 289 and 222 nm. Typical unfolding curves are shown in Figures 4(A) and (B). The dead-time event is almost negligible in this denaturant concentration range, and all unfolding kinetics are monophasic and can be adequately fitted to a single exponential process.

The far-UV CD burst-phase amplitude, obtained by extrapolation of the refolding curve to zero time, and final CD values of refolding at long time are plotted in Figure 5(A) as a function of GdnCl concentration. The burst-phase amplitude deviates markedly from the far-UV CD ellipticity expected for the fully unfolded protein at GdnCl concentration below 3 M. Because the burst phase and the subsequent folding phases are kinetically uncoupled, the sigmoidal character of the burst-phase amplitude provides strong evidence of an unresolved rapid folding event that leads to the formation of a burst-phase intermediate.[35,36] To characterize the nature of the burst-phase intermediate populated rapidly during refolding in more detail, we measured the refolding kinetics by near-UV CD at various wavelengths, and the spectrum of the burst-phase intermediate was constructed from the amplitude change within the dead time as a function of the wavelength. The CD

spectra of the burst phase obtained are compared with the spectra of the native state and the equilibrium unfolded state in Figure 5(B). It can be seen that the near-UV CD spectra of the burst phase almost coincide with that of the unfolded state in 6 M GdnCl. This result indicates that the tight packing in the tertiary structure around the aromatic residues of hen lysozyme is not yet fully formed within the first 10 ms of refolding.

Two-State Analysis

The apparent rate constants (k_{obs}) of refolding and unfolding reactions were obtained by fitting the observed reaction curves with Eq. 1. The plot of the denaturant dependence of the observed rate, so-called chevron plot, is shown in Figure 6(A). If the folding-unfolding kinetics at pH 2.2 and 25°C is described by a simple two-state process (N↔U), the apparent rate constant is equal to the sum of the microscopic rate constants of refolding and unfolding, k_f and k_U:

$$k_{obs} = k_f + k_U \tag{6}$$

It is widely assumed that ln k_f and ln k_U depend linearly on denaturant concentration c, and consequently the GdnCl dependence of ln k_{obs} shows a V-shaped profile.[37] The data in Figure 6(A) were fitted by assuming the linear dependence of ln k_f and ln k_U on GdnCl concentration c:

$$\ln k_{f,u} = \ln k^0_{f,u} + (m^{\ddagger}_{f,u}/RT)c \tag{7}$$

$$\ln k_{obs} = \ln[\exp\{\ln k^0_f + (m^{\ddagger}_f/RT)c\} + \exp\{\ln k^0_u + (m^{\ddagger}_u/RT)c\}] \tag{8}$$

where k^0_u and k^0_f are the unfolding and refolding rate constants in the absence of GdnCl, and $m^{\ddagger}_{f,u}$ are the corresponding slopes. The $m^{\ddagger}_{f,u}$ values are interpreted as the changes in solvent accessibility associated with formation of the transition state in the refolding or unfolding reaction. In the case of a simple two-state mechanism, ln k_f can be deduced from the $m^{\ddagger}_u$ value of the unfolding kinetics and m_{NU} value from the equilibrium unfolding data[37]:

$$\ln k_f = \ln k^0_f + \{(m^{\ddagger}_u - m_{NU})/RT\}c \tag{9}$$

The continuous curve in Figure 6(A) shows the theoretical curve based on Eq. 8. On the other hand, the dot line represents that calculated for an ideal two-state system using Eq. 9. The rate constants of refolding observed experimentally deviate considerably from the dot line calculated for an ideal two-state system. This deviation from the expected two-state model is easily explained by the presence of burst-phase species observed under the refolding conditions.

DISCUSSION

In the present study, we have investigated the search for a possible intermediate state in hen lysozyme by equilibrium and kinetic experiments using static and stopped-flow CD spectroscopy under the acidic conditions. We discuss below the role and significance of the early kinetic intermediate in hen lysozyme folding and its possible relationship with the partially folded equilibrium intermediate.

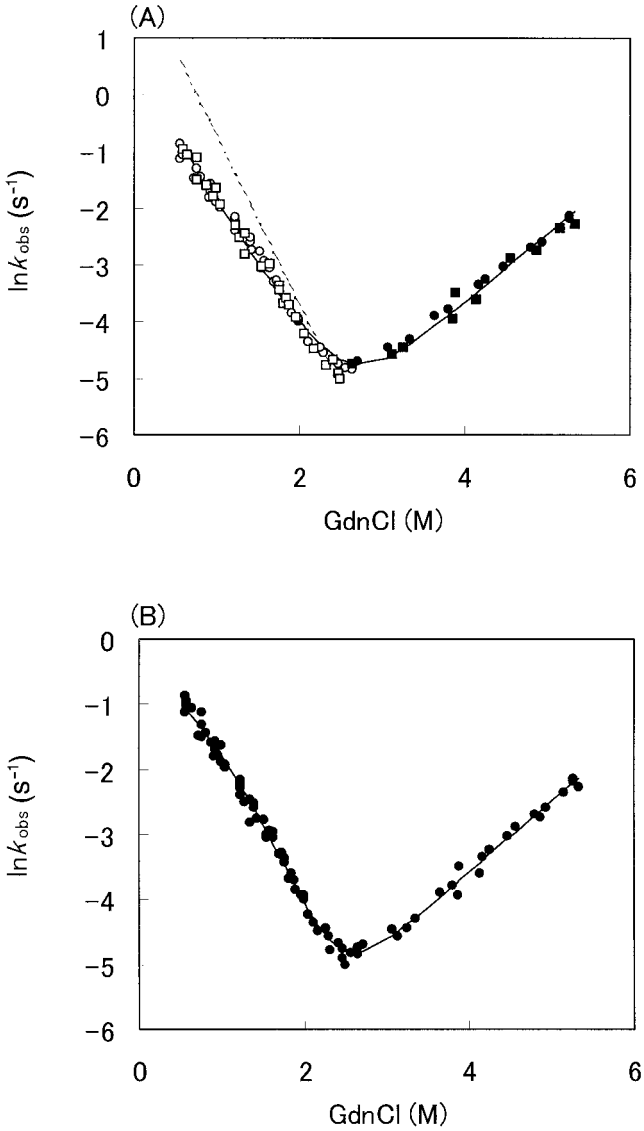

Fig. 6. **A:** GdnCl concentration dependence of the apparent rate constants of the refolding (open symbols) and unfolding (filled symbols) reactions of hen lysozyme measured at pH 2.2 by CD at 222 nm (circles), and 289 nm (squares). The continuous line is the best fit of the data to Eq. 8, which describes a two-state transition. The dotted line shows the predicted data for a two-state transition according to Eq. 9, in which 10.57 kJ/mol in Table I was used as m_{NU} value. **B:** GdnCl concentration dependence of the folding and unfolding kinetics of hen lysozyme. Filled circles denote the experimental k_{obs} measured by CD at 222 and 289 nm. The continuous line is the best fit of the data to Eq. 11 assuming the on-pathway model.

On-Pathway (Sequential) Model by Three-State Analysis

Because the observation of a burst phase indicates the presence of at least one intermediate in the lysozyme-folding reaction, an analysis of the data using a sequential three-state model as minimal kinetic mechanism may be useful to detect a possible effect of an intermediate on the kinetic data.

$$\text{(On-pathway model)} \quad \mathrm{U} \underset{k_{IU}}{\overset{k_{UI}}{\Leftrightarrow}} \mathrm{I} \underset{k_{NI}}{\overset{k_{IN}}{\Leftrightarrow}} \mathrm{N}$$

Because the observable kinetics occur on a much slower timescale than the burst phase, the burst-phase intermediate (I) and unfolded (U) states are assumed to equilibrate with each other within the dead time of stopped-flow experiments[36,38]; the rate constants for conversion between I and U are much larger than those between I and N, which limit the rate of folding. In this scheme, the burst-phase intermediate (I) is thought to represent an ensemble of compact states with native-like secondary structure and assumed to be an obligatory intermediate on a direct path from U to N. Under these assumptions, the observed rate constant is described as follows.

$$k_{obs} = k_{IN} \times \{(1/(1 + K_{IU}))\} + k_{NI} \quad (10)$$

where K_{IU} represents the preequilibrium constant between the burst-phase intermediate and unfolded states. This preequilibrium allows the transition curve of the burst-phase amplitude versus GdnCl concentration to be interpreted as an unfolding transition for the intermediate. The three values $\ln(k_{IN})$, $\ln(k_{NI})$, and $\ln(K_{IU})$ are presumed to vary linearly with GdnCl concentration. Finally, the following equation for the observed rate constant, together with the associated amplitude of the burst phase, is used to fit the kinetic chevron plot:

$$\begin{aligned} k_{obs} = {} & \exp\{\ln k^0_{IN} + (m^{\ddagger}_{IN}/RT)c\} \\ & \times [1/\{1 + \exp\{-(\Delta G^0_{IU} - m_{IU}c)/RT\}] \\ & + \exp\{\ln k^0_{NI} + (m^{\ddagger}_{NI}/RT)c\} \end{aligned} \quad (11)$$

where $m^{\ddagger}_{ij}$ represents the dependence on GdnCl concentration of the rate constant k_{ij} (i and j stand for N, I, or U), and k^0_{ij} is the rate constant in the absence of denaturant.

The observed burst-phase amplitude (X_{obs}) at any concentration of GdnCl is given by the following equation according to a two-state model:

$$\begin{aligned} X_{obs}(c) = {} & [X_I + X_U \exp\{-(\Delta G^0_{IU} - m_{IU}c)/RT\}] \\ & \div [1 + \exp\{-(\Delta G^0_{IU} - m_{IU}c)/RT\}] \end{aligned} \quad (12)$$

where X_I and X_U are ellipticity values in the I and U states, respectively, and it is also assumed that $X_I = b_1 + b_2 c$ and $X_U = b_3 + b_4 c$. With regard to b_3 and b_4, we used the values (a_3 and a_4) obtained in the fitting in Figure 1(A). In the analysis, thus, the model contains eight independent parameters (k^0_{IN}, $m^{\ddagger}_{IN}$, k^0_{NI}, $m^{\ddagger}_{NI}$, ΔG^0_{IU}, m_{IU} and b_1, b_2); these were varied systematically to fit the observed burst-phase amplitude and rates. The kinetic parameters corresponding to the best simultaneous fit for all rate constants and preequilibrium data are listed in Table II. The continuous line in Figure 5(A) represents the theoretical curve (Eq. 12) drawn with the parameter values obtained based on the on-pathway model in Table II. The denaturant dependence of the apparent rate constants (k_{obs}) for folding and unfolding (i.e., chevron plot) is shown in Figure 6(B) again, including the fitting curve to the on-pathway model. We can see the reasonable agreement between the experimental data and the theoretical curves.

TABLE II. Parameters From the Fits of the Hen Lysozyme Kinetic Data to On-Pathway and Off-Pathway Models at pH 2.2

	On-Pathway	Off-Pathway
k^0_{IN} (s^{-1})	0.78 (0.04)	
$m^{\ddagger}_{IN}$ (kJ/mol/M)	−2.98 (0.09)	
k^0_{UN} (s^{-1})		17.92 (0.82)
$m^{\ddagger}_{UN}$ (kJ/mol/M)		−8.58 (0.09)
k^0_{NI} (s^{-1})	$3.55\ (0.05) \times 10^{-4}$	
$m^{\ddagger}_{NI}$ (kJ/mol/M)	2.70 (0.07)	
k^0_{NU} (s^{-1})		$3.54\ (0.40) \times 10^{-4}$
$m^{\ddagger}_{NU}$ (kJ/mol/M)		2.71 (0.07)
ΔG^0_{IU} (kJ/mol)	7.78 (1.32)	7.78 (1.12)
m_{IU} (kJ/mol/M)	5.61 (0.29)	5.60 (0.25)
ΔG^0_{NU} (kJ/mol)[a]	26.85 (1.46)	26.85 (0.49)
m_{NU} (kJ/mol/M)[a]	11.28 (0.45)	11.29 (0.16)

[a]The parameters were calculated by using the values from the best fits to the kinetic data. For the on-pathway model $\Delta G^0_{NU} = \Delta G^0_{IU} + (-RT \ln (k^0_{NI}/k^0_{IN}))$ and $m_{NU} = m^{\ddagger}_{NI} - m^{\ddagger}_{IN} + m_{IU}$. For the off-pathway model $\Delta G^0_{NU} = -RT \ln(k^0_{NU}/k^0_{UN})$ and $m_{NU} = m^{\ddagger}_{NU} - m^{\ddagger}_{UN}$.

It is well known that the chevron plots of various proteins exhibiting intermediate states deviate markedly from the expected linear plot (so-called rollover) where the observed rate of folding levels off.[9,10] In this study, we could observe the slight rollover due to the high stability of the intermediate state (see Fig. 6). That is, at lower GdnCl concentration, the U↔I equilibrium lies toward I, and the observable folding rate approaches k_{IN} (Eq. 10), which limits the rate of formation of N. The validity of the on-pathway model is supported by the good agreement between the parameters calculated by using the kinetic data [ΔG^0_{NU} = 26.85 (1.49) kJ/mol, m_{NU} = 11.28 (0.45) kJ/mol/M, and m_{IU} = 5.61 (0.29) kJ/mol/M], and the values from the best fit to the equilibrium unfolding data under identical or more acidic conditions (ΔG^0_{NU} = 24.22 (0.6) kJ/mol, m_{NU} = 10.57 (0.25) kJ/mol/M, and m_{IU} = 5.07 (1.88) kJ/mol/M) (Table I). Consequently, the kinetics of folding and unfolding of hen lysozyme under the acidic condition can be described quantitatively on the basis of a sequential three-state mechanism with an early well-populated folding intermediate.

Triangular Model

The point we must address is that the idea of parallel folding pathway (fast-track and slow-track) has been developed in refolding of hen lysozyme as a triangular model under the neutral pH condition.[23,26] The triangular mechanism is composed of two parallel processes, a direct transition from U to N and a sequential pathway from U to N via I. This parallel folding reaction has been attributed to the kinetic partitioning that occurs rapidly after folding is initiated and that gives the molecules the chance to enter the direct pathway or a slow folding pathway.[26,39] In the triangular model, within the first few milliseconds, fully native molecules may be formed on a direct pathway

without the occurrence of any kinetic intermediate. In that case, a fraction of the ensemble of unfolded molecules is converted directly to the native state in a very fast process, whereas the rest of molecules adopt the native conformation with much slower kinetics. However, our kinetic data obtained under the acidic condition show that the burst-phase amplitude extrapolated to time zero at the near-UV region approaches the signal expected for the unfolded state in 6 M GdnCl [Fig. 5(B)], suggesting that virtually all molecules convert from the unfolded state into the burst-phase species and follow the same kinetic route. On this basis we did not conduct the kinetic analysis based on a triangular folding model.

Off-Pathway Model

In addition to the sequential folding mechanism with an obligatory intermediate, one can consider an alternative three-state mechanism, the so-called off-pathway mechanism.[9] The off-pathway mechanism implies that the intermediate contains non-native interactions, which have to be disrupted before folding can proceed.

$$\text{(Off-pathway model)} \quad \mathrm{I} \underset{k_{\mathrm{UI}}}{\overset{k_{\mathrm{IU}}}{\Leftrightarrow}} \mathrm{U} \underset{k_{\mathrm{NU}}}{\overset{k_{\mathrm{UN}}}{\Leftrightarrow}} \mathrm{N}$$

The apparent rate constant of the refolding and unfolding reactions is represented by the following equation:

$$k_{\mathrm{obs}} = k_{\mathrm{UN}} \times \{(K_{\mathrm{IU}}/(1 + K_{\mathrm{IU}}))\} + k_{\mathrm{NU}} \tag{13}$$

$$k_{\mathrm{obs}} = \exp\{\ln k^0_{\mathrm{UN}} + (m^{\ddagger}_{\mathrm{UN}}/RT)c\} \times [\exp\{-(\Delta G^0_{\mathrm{IU}} - m_{\mathrm{IU}}c)/RT\}/\{1 + \exp\{-(\Delta G^0_{\mathrm{IU}} - m_{\mathrm{IU}}c)/RT\}\}] + \exp\{\ln k^0_{\mathrm{NU}} + (m^{\ddagger}_{\mathrm{NU}}/RT)c\} \tag{14}$$

This model fits the experimental data as well as the on-pathway model (the resulting parameters are shown in Table II). Although the stability and m values of the intermediate and native states are unchanged in fitting to the on- and off-pathway models, the difference between the two models lies in the rate of folding to the native state (see Table II). Namely, the rate constant (k_{UN}) for direct folding from U to N based on the off-pathway model shows much steeper dependence on c than k_{IN} for the folding from I to N based on the on-pathway model. As a consequence, the kinetic analysis using the three-state model cannot readily discriminate between the on-pathway and off-pathway when the intermediate state forms within the dead time (~ms) of stopped-flow experiments.[36,38] Instead, our data analysis using the on-pathway model show that the rapid step from the unfolded state to the burst-phase intermediate is a good approximation to a two-state process, and the parameter (ΔG^0_{IU} = 7.78 kJ/mol and m_{IU} = 5.61 kJ/mol/M) determined kinetically are fairly compatible with the equilibrium thermodynamic parameters (ΔG^0_{IU} = 5.07 kJ/mol and m_{IU} = 5.07 kJ/mol/M) observed at pH 0.9, if we take into consideration the different pH condition and experimental uncertainty. This comparison strongly suggests the similarity between the acidic equilibrium intermediate state and the burst-phase refolding intermediate. Although the possibility of an off-pathway model cannot be excluded by the kinetic data, we consider such a mechanism highly unlikely.

Comparison of the Folding Behaviors of Hen Egg-White Lysozyme Under Acidic and Neutral pH Conditions

As described in Introduction, complicated kinetics with the overshoot in the refolding of hen lysozyme have been observed by the far-UV CD under neutral pH conditions.[15,18] Substantial quenching of tryptophan fluorescence was also observed during the fast phase.[19,22] The excess ellipticity in the far-UV CD and unusual fluorescence quenching are thought to result from contributions from disulfide bonds or aromatic residues in non-native conformations, possibly involving either Trp62 and/or Trp108.[19,25] These results support the view that the rate-determining step in the slow phase involves structural reorganization in the formation of the native state. In this study, when the pH is lowered to 2.2, substantial differences are shown in the kinetic refolding behavior of this protein. That is, the overshoot in the far-UV CD observed at neutral pH is not observed; there are presumably less non-native interactions that can hamper folding toward the native state. In addition, at this reduced pH the folding/unfolding rates are remarkably slower than those at neutral pH, and the lifetime of the burst-phase species is much longer than that at the well-studied higher pH values.[31] Although we cannot rule out the existence of some non-native interactions in the transient intermediate, this lower pH condition allowed us to characterize a rapidly formed burst-phase intermediate and the folding process from the burst-phase intermediate state to the native state with a single exponential process. As a result, all the data in this study indicate that the folding pathway of this protein under the acid condition can be modeled quantitatively on the basis of a sequential three-state mechanism with a well-populated early folding intermediate.

However, sequential folding is not the only model for interpreting the presence of the folding intermediate. Previous data on the folding reactions of this protein under the neutral pH conditions have been explained by a triangular three-state mechanism.[23,26] These results raise the intriguing possibility that this protein in the neutral and acidic pH conditions could fold with different mechanisms. It may not be surprising that the proportion of molecules that follow fast (U→N) and slow (U→I→N) routes to the native state changes with pH. However, in this study, we have shown that the equilibrium intermediate state observed at pH 0.9 is compatible with the burst-phase intermediate in the kinetic refolding reaction. Whether the intermediate state can be detected at equilibrium is dependent on the relative stability among the native, intermediate, and unfolded states.[13] The apparent difference in the equilibrium unfolding at pH 0.9 and 2.2 is probably due to the difference in the relative stability of the native state to the intermediate. The result suggests that the relative stability of the intermediate state of this

protein may play a critical role in determining the apparent folding behavior of this protein. Namely, if the stability of the intermediate state in determining the pathway is marginal under the neutral pH condition, it accumulates only partially even under native conditions. In such a case, the folding reaction could be explained by either two-state or three-state model, and a triangle folding mechanism could be applied to the folding reaction.[38] At present, although it is still unclear which mechanisms (sequential or triangular model) are predominant earlier during the folding reaction, the present results suggest that the sequential three-state mechanism is the basis for understanding the folding reaction of hen egg-white lysozyme. In addition, the experimental data in this study highlight the importance of searching a wide range of pH conditions by a combination of diverse techniques. For example, the present study does not detect the direct channel (U→N) in the near-UV range. Stopped-flow fluorescence measurements are much more sensitive and would clarify whether folding at pH 2.2 truly follows a fundamentally different mechanism compared to that observed at higher pH.

Folding Behavior of Lysozyme and α-Lactalbumin

For several globular proteins, including α-lactalbumin, Ca^{2+}-binding lysozyme, cytchrome c, apomyoglobin, ribonuclease H1, and others, partially folded equilibrium intermediate are populated under mildly denaturing conditions and are characterized as molten globules.[2,4] The general structural features of these equilibrium molten globule states were reported to be similar to those found in early kinetic intermediates, supporting the sequential folding model, which assumes that the native structure is formed in a hierarchical way along a linear pathway.[1,2,4] Comparison of the folding behavior of the lysozyme and α-lactalubumin families, which have evolved from a common ancestor,[40] is particularly useful for understanding the folding mechanism. The lysozyme and α-lactalubumin family is divided into three groups: α-lactalubumin, Ca^{2+}-binding lysozyme, and conventional (non-Ca^{2+}-binding) lysozyme.[41] Previous studies of homologous α-lactalbumin and Ca^{2+}-binding lysozyme using CD spectroscopy have shown a close similarity between the early transient intermediate formed within the stopped-flow dead time and the equilibrium molten globule state.[35,38,42] These results for bovine α-lactalbumin and Ca^{2+}-binding lysozyme confirm the sequential model for protein folding with the molten globule state as an obligatory folding intermediate. In this study, we have shown that the folding and unfolding kinetics of hen egg-white lysozyme under the acidic pH condition can be described quantitatively by a linear three-state model and that the equilibrium intermediate state observed at pH 0.9 is compatible with the burst-phase intermediate in the kinetic refolding reaction. This finding suggests that the intermediate formation is a general step and that there is no fundamental distinction in protein folding among the lysozyme and α-lactalbumin family.

Thermodynamic Characterization of the Intermediate and Transition States of Hen Lysozyme

In the refolding of lysozyme and α-lactalbumin, which contain disulfide bonds, the burst-phase intermediates with a native-like helical structure under refolding conditions are significantly more compact than completely unfolded polypetide chains.[27,31,43] During refolding, collapse of the protein structure may be concomitant with, or may precede, such secondary structure formation.[44,45] The environment produced by this collapse is likely to be hydrophobic in nature and may help to generate or stabilize secondary structure, which is supported by a significant change in the m value of this reaction. The hydrophobically collapsed state that is formed within the stopped-flow dead time of the folding process of hen lysozyme has been suggested to have properties characteristic of equilibrium molten globule states.[13,14] Thus, detailed knowledge of structures of the burst-phase intermediates is essential for understanding how a protein's fold is determined without extensive side-chain-packing interactions. For application to the protein-folding pathway, the thermodynamic characterization of this compact non-native state should provide important information on whether the transient intermediate (molten globule) state can be characterized as an independent thermodynamic state on the pathway of protein folding or rather some solvent-dependent modification of the still unfolded polypeptide chain or transient aggregates in protein folding.[4,46–50]

According to the recent study on homologous α-lactalbumin,[51] the formation of a compact intermediate state from the unfolded state proceeds with a negative heat capacity change, a positive enthalpy change, and is dominated by a positive entropy change, deriving from hydrophobic collapse and massive dehydration of the protein groups partially shielded from solvent water on folding. Whether the unfolding from the intermediate (molten globule) state is cooperative may depend on how much native-like specific structure is organized in this state, and the more native-like the intermediate is, the more cooperative the unfolding transition may be.[2] In this respect, a good correlation of the stability and the unfolding cooperativity of the molten globule states has been shown in the study of chimeric proteins of bovine and human α-lactalbumin.[52] In this study, the denaturant dependence of the burst-phase amplitude, which defines the equilibrium between the unfolded and intermediate states, fits well to a two-state transition model as shown by the continuous line in Figure 5(A). This result provides strong evidence that the burst-phase intermediate of hen lysozyme is a distinct thermodynamic state (ensemble of compact conformations) on the folding pathway.

The proportionality between structural changes and m values has allowed a crude determination of the extent of structure in the burst-phase intermediate and the transition state. Thus, as a quantitative measure of the compactness of the burst-phase intermediate and the transition state, it is useful to consider the two values; $\alpha_I = m_{IU}/m_{NU}$ and $\alpha_{\ddagger} = 1 - (m^{\ddagger}_{NI}/m_{NU})$. Particularly, comparison of the

TABLE III. The Relative Degree of Structural Organization in the Intermediate and the Transition States

	$\alpha_I = m_{IU}/m_{NU}$ (%)	$\alpha_‡ = 1 - m^‡_{NI}/m_{NU}$ (%)
Hen egg-white lysozyme	50 (5)	76 (2)
Equine lysozyme	36 (6)[a]	83 (1)[a]
Bovine α-lactalbumin	31[a]	52[a]

[a]Mizuguchi et al., 1998.

relative degrees of structural organization (α_I and $\alpha_‡$) among hen lysozyme, bovine α-lactalbumin and Ca^{2+}-binding equine lysozyme is important for understanding the folding mechanism of the lysozyme and α-lactalbumin family.[38] Table III contains the α_I and $\alpha_‡$ values of these proteins. The results show that the α_I (50%) of hen lysozyme is much larger than those of α-lactalbumin and equine lysozyme, suggesting that the interactions stabilizing the intermediate (molten globule) state of hen lysozyme are more extensive and cooperative. This higher α_I value of hen lysozyme may be attributed to be the tight packing at the interface between the α and β domains.[53]

It has been shown that the overall topology of the intermediate (molten globule) state of the structurally related α-lactalbumin is native-like, particularly in the α-domain.[54,55] In conjunction with our present observations, this finding suggests that the native-like topology is formed at the early stage in the folding process of hen lysozyme before the formation of the native structure. With this in mind, the slow step from the burst-phase intermediate state to the native state, which is highly cooperative, appears to reflect the specific change to its rigid close-packed structure within a compact ensemble with a native-like topology. The $\alpha_‡$ value of hen lysozyme is 75% much higher than the α_I value. This result shows that the transition state of hen lysozyme is much more organized than the intermediate state, supporting the on-pathway model in which interactions formed in the intermediate state persist in the transition and native states.

CONCLUSION

In this study, we have shown that the folding and unfolding kinetics of hen egg-white lysozyme under the acidic condition can be described quantitatively by a linear three-state model and that the equilibrium intermediate state observed at pH 0.9 is compatible with the burst-phase intermediate in the kinetic refolding reaction. The present results, together with the known results for Ca^{2+}-binding lysozyme and α-lactalbumin, suggest that the stability of the intermediate states may play a critical role in determining the apparent folding behavior of a globular protein. That is to say, the higher stability of the intermediate state of hen lysozyme requires this protein to obey the sequential folding model, in which an intermediate state accumulates as a consequence of its intrinsic stability before the formation of the native state.

ACKNOWLEDGMENTS

The authors thank Dr. Mizuguchi for helpful comments and advice on this project and Dr. P. McPhie and Dr. D. Hall, whose criticisms of the style and form of the manuscript led to considerable improvement in the clarity of expression.

REFERENCES

1. Kim PS, Baldwin RL. Intermediates in the folding reactions of small proteins. Annu Rev Biochem 1990;59:631–660.
2. Arai M, Kuwajima K. Role of the molten globule state in protein folding. Adv Protein Chem 2000;53:209–282.
3. Chamberlain AK, Marqusee S. Comparison of equilibrium and kinetic approaches for determining protein folding mechanisms. Adv Protein Chem 2000;53:283–328.
4. Ptitsyn OB. Molten globule and protein folding. Adv Protein Chem 1995;47:83–229.
5. Jackson SE. How do small single-domain protein fold? Fold Design 1998;3:R81–R91.
6. Dill KA, Chan HS. From levinthal to pathways to funnels. Nat Struct Biol 1997;4:10–19.
7. Shakhnovich EI. Theoretical studies of protein folding thermodynamics and kinetics. Curr Opin Struct Biol 1997;7:29–40.
8. Creighton TE. The energetic ups and downs of protein folding. Nat Struct Biol 1994;1:135–138.
9. Baldwin RL. On-pathway versus off-pathway folding intermediates. Fold Design 1996;1:R1–R8.
10. Roder H, Colon W. Kinetic role of early intermediates in protein folding. Curr Opin Struct Biol 1997;7:15–28.
11. Tanford C, Aune KC, Ikai A. Kinetics of unfolding and refolding of proteins. 3. Results for lysozyme. J Mol Biol 1973;73:185–197.
12. Kato S, Okamura M, Shimamoto N, Utiyama H. Spectral evidence for a rapidly formed structural intermediate in the refolding kinetics of hen egg-white lysozyme. Biochemistry 1981;20:1080–1085.
13. Kuwajima K, Hiraoka Y, Ikeguchi M, Sugai S. Comparison of the transient folding intermediates in lysozyme and α-lactalbumin. Biochemistry 1985;24:874–881.
14. Ikeguchi M, Kuwajima K, Mitani M, Sugai S. Evidence for identity between the equilibrium unfolding intermediate and a transient folding intermediate: a comparative study of the folding reactions of α-lactalbumin and lysozyme. Biochemistry 1986;25:6965–6972.
15. Chaffotte AF, Guillou Y, Goldberg ME. Kinetic resolution of peptide bond and side chain far-UV circular dichroism during the folding of hen egg white lysozyme. Biochemistry 1992;31:9694–9702.
16. Miranker A, Radford SE, Karplus M, Dobson CM. Demonstration by NMR of folding domains in lysozyme. Nature 1991;349:633–636.
17. Miranker A, Robinson CV, Radford SE, Aplin RT, Dobson CM. Detection of transient protein folding populations by mass spectrometry. Science 1993;262:896–900.
18. Radford SE, Dobson CM, Evans PA. The folding of hen lysozyme involves partially structured intermediates and multiple pathways. Nature 1992;358:302–307.
19. Denton ME, Rothwarf DM, Scheraga HA. Kinetics of folding of guanidine-denatured hen egg white lysozyme and carboxymethyl (Cys^6, Cys^{127})-lysozyme: a stopped-flow absorbance and fluorescence study. Biochemistry 1994;33:11225–11236.
20. Itzhaki LS, Evans, PA, Dobson CM, Radford SE. Tertiary interactions in the folding pathway of hen lysozyme: kinetic studies using fluorescent probes. Biochemistry 1994;33:5212–5220.
21. Matagne A, Radford SE, Dobson CM. Fast and slow tracks in lysozyme folding: insight into the role of domains in the folding process. J Mol Biol 1997;267:1068–1074.
22. Matagne A, Chung EW, Ball LJ, Radford SE, Robinson CV, Dobson CM. The origin of the α-domain intermediate in the folding of hen lysozyme. J Mol Biol 1998;277:997–1005.
23. Kiefhaber T. Kinetic traps in lysozyme folding. Proc Natl Acad Sci USA 1995;92:9029–9033.
24. Gladwin ST, Evans PA. Structure of very early protein folding intermediates: new insight through a variant of hydrogen exchange labeling. Fold Design 1996;1:407–417.
25. Rothwarf DM, Scheraga HA. Role of non-native aromatic and

hydrophobic interactions in the folding of hen egg white lysozyme. Biochemistry 1996;35:13797–13807.
26. Wildegger G, Kiefhaber T. Three-state model for lysozyme folding: triangular folding mechanism with an energetically trapped intermediate. J Mol Biol 1997;270:294–304.
27. Segel DJ, Bachmann A, Hofrichter J, Hodgson KO, Doniach S, Kiefhaber T. Characterization of transient intermediates in lysozyme folding with time-resolved small-angle x-ray scattering. J Mol Biol 1999;288:489–499.
28. Bai Y. Kinetic evidence of an on-pathway intermediate in the folding of lysozyme. Protein Sci 2000;9:194–196.
29. Sasahara K, Demura M, Nitta K. Partially unfolded equilibrium state of hen lysozyme studied by circular dichroism spectroscopy. Biochemistry 2000;39:6475–6482.
30. Sasahara K, Sakurai M, Nitta K. Pressure effect on denaturant-induced unfolding of hen egg white lysozyme. Proteins 2001;44: 180–187.
31. Chen L, Wildegger G, Kiefhaber T, Hodgson KO, Doniach S. Kinetics of lysozyme refolding: structural characterization of a non-specifically collapsed state using time-resolved x-ray scattering. J Mol Biol 1998;276:225–237.
32. Nozaki Y. The preparation of guanidine hydrochloride. Methods Enzymol 1972;26:43–50.
33. Pace CN. Determination and analysis of urea and guanidine hydrochloride denaturation curves. Methods Enzymol 1986;131: 266–280.
34. Santoro MM, Bolen DW. Unfolding free energy changes determined by the linear extrapolation method. 1. Unfolding of phenylmethanesulfonyl α-chymotrypsin using different denaturants. Biochemistry 1988;27:8063–8068.
35. Arai M, Kuwajima K. Rapid formation of a molten globule intermediate in refolding of α-lactalbumin. Fold Design 1996;1: 275–287.
36. Khorasanizadeh S, Peters ID, Roder H. Evidence for a three-state model of protein folding from kinetic analysis of ubiquitin variants with altered core residues. Nat Struct Biol 1996;3:193–205.
37. Matouschek A, Kellis JT Jr, Serrano L, Bycroft M, Fersht AR. Transient folding intermediates characterized by protein engineering. Nature 1990;346:440–445.
38. Mizuguchi M, Arai M, Ke Y, Nitta K, Kuwajima K. Equilibrium and kinetics of the folding of equine lysozyme studied by circular dichroism spectroscopy. J Mol Biol 1998;283:265–277.
39. Matagne A, Dobson CM. The folding process of hen lysozyme: a perspective from the "new view." Cell Mol Life Sci 1998;54:363–371.
40. Mckenzie HA, White FH Jr. Lysozyme and α-lactalbumin: structure, function, and interrelationship. Adv Protein Chem 1991;41: 173–315.
41. Nitta K, Sugai S. The evolution of lysozyme and α-lactalbumin. Eur J Biochem 1989;182:111–118.
42. Haezebrouck P, Noyelle K, Van Dael H. Equilibrium and kinetic folding of pigeon lysozyme. Biochemistry 1998;37:6772–6780.
43. Gast K, Zirwer D, Muller-Frohne M, Damaschun G. Compactness of the kinetic molten globule of bovine alpha-lactalbumin: a dynamic light scattering study. Protein Sci 1998;7:2004–2011.
44. Hooke SD, Radford SE, Dobson CM. The refolding of human lysozyme: a comparison with the structurally homologous hen lysozyme. Biochemistry 1994;33:5867–5876.
45. Morgan CJ, Miranker A, Dobson CM. Characterization of collapsed states in the early stages of the refolding of hen lysozyme. Biochemistry 1998;37:8473–8480.
46. Kuwajima K. The molten globule state of α-lactalbumin. FASEB J 1996;10:102–109.
47. Pfeil W. Is the molten globule a third thermodynamic state of protein? The example of α-lactalbumin. Proteins 1998;30:43–48.
48. Sosnick TR, Shtilerman MD, Mayne L, Englander SW. Ultrafast signals in protein folding and the polypeptide contracted state. Proc Natl Acad Sci USA 1997;94:8545–8550.
49. Silow M, Oliveberg M. Transient aggregates in protein folding are easily mistaken for folding intermediates. Proc Natl Acad Sci USA 1997;94:6084–6086.
50. Ikeguchi M, Fujino M, Kato M, Kuwajima K, Sugai S. Transition state in the folding of α-lactalbumin probed by the 6–120 disulfide bond. Protein Sci 1998;7:1564–1574.
51. Griko YV, Freire E, Privalov G, Van Dael H, Privalov PL. The unfolding thermodynamics of c-type lysozyme: a calorimetric study of the heat denaturation of equine lysozyme. J Mol Biol 1995;252:447–459.
52. Mizuguchi M, Masaki K, Demura M, Nitta K. Local and long-range interactions in the molten globule state: a study of chimeric proteins of bovine and human α-lactalbumin. J Mol Biol 2000;298: 985–995.
53. Griko YV. Energetic basis of structural stability in the molten globule state: α-lactalbumin. J Mol Biol 2000;297:1259–1268.
54. Wu LC, Kim PS. A specific hydrophobic core in the α-lactalbumin molten globule. J Mol Biol 1998;280:175–182.
55. Song J, Bai P, Luo L, Peng Z-Y. Contribution of individual residues to formation of the native-like tertiary topology in the α-lactalbumin molten globule. J Mol Biol 1998;280:167–174.